Oncogenic Kras Requires Simultaneous PI3K Signaling to Induce ERK Activation and Transform Thyroid Epithelial Cells *In vivo*

Kelly A. Miller,[1] Nicole Yeager,[1] Kristen Baker,[4] Xiao-Hui Liao,[2] Samuel Refetoff,[2,3] and Antonio Di Cristofano[1,4]

[1]Human Genetics Program, Fox Chase Cancer Center, Philadelphia, Pennsylvania; Departments of [2]Medicine and [3]Pediatrics and Committee on Genetics, University of Chicago, Chicago, Illinois; and [4]Department of Developmental and Molecular Biology, Albert Einstein College of Medicine, Bronx, New York

Abstract

Thyroid tumors arising from the follicular cells often harbor mutations leading to the constitutive activation of the PI3K and Ras signaling cascades. However, it is still unclear what their respective contribution to the neoplastic process is, as well as to what extent they interact. We have used mice harboring a *Kras* oncogenic mutation and a *Pten* deletion targeted to the thyroid epithelium to address *in vivo* these questions. Here, we show that although each of these two pathways, alone, is unable to transform thyroid follicular cells, their simultaneous activation is highly oncogenic, leading to invasive and metastatic follicular carcinomas. In particular, phosphatidylinositol-3-kinase (PI3K) activation suppressed Kras-initiated feedback signals that uncouple mitogen-activated protein kinase (MAPK)/extracellular signal-regulated kinase (ERK) kinase (MEK) and ERK activation, thus stunting MAPK activity; in addition, PI3K and Kras cooperated to drastically up-regulate cyclin D1 mRNA levels. Finally, combined pharmacologic inhibition of PI3K and MAPK completely inhibited the growth of double-mutant cancer cell lines, providing a compelling rationale for the dual targeting of these pathways in thyroid cancer. [Cancer Res 2009;69(8):3689–94]

Introduction

Activating mutations of Ras family members are common in thyroid cancer originating from the follicular epithelium (1). Several transgenic approaches have been used in the past to define the molecular mechanisms of Ras-mediated thyroid transformation (2, 3). However, it is now clear that supraphysiologic expression often results in phenotypes that do not really model the activity of oncogenic Ras expressed at endogenous levels (4). The development of mouse strains that more faithfully reproduce the expression of mutant Ras seen in human cancers has recently allowed a more accurate analysis of the mechanisms involved in tumor development and progression, and of Ras cross-talk with cooperating oncogenic alterations (5, 6).

Aberrant activation of the phosphatidylinositol-3-kinase (PI3K)/AKT pathway plays an extensive role in thyroid tumorigenesis, particularly in follicular (55%) and anaplastic thyroid cancer (58%), and promotes progression of benign adenomas to follicular thyroid cancer and to anaplastic thyroid cancer as the genetic alterations of this pathway accumulate (7, 8). Furthermore, the frequencies and overlap of genetic alterations in the PI3K and Ras/mitogen-activated protein kinase (MAPK) cascades increase with progression from differentiated to undifferentiated thyroid tumors: alterations in PI3K and MAPK pathways occur in nearly all high-grade tumors, with the majority of the cases harboring genetic alterations in both pathways (8). To understand how PI3K activation cooperates with activation of Ras in promoting thyroid cancer pathogenesis, we have used an *in vivo* approach in genetically defined mouse models.

Materials and Methods

Animals and treatments. The $Kras^{LSL}$, $Pten^{L/L}$, and thyroid peroxidase promoter (TPO)-Cre strains have been described (9–11). All strains were backcrossed in the 129Sv background for at least eight generations. LY294002 (Cayman Chemical) was injected i.p. at 25 mg/kg body weight twice a week, starting at age 3 wk.

Hormone measurements. Blood was collected by cardiac puncture. Serum thyroid-stimulating hormone (TSH) was measured using a sensitive, heterologous, disequilibrium double-antibody precipitation RIA (12), and results were expressed in mU/liter. All samples were individually analyzed for each mouse. Total T4 concentrations were measured by a solid-phase RIA (Coat-a-Count; Diagnostic Products Corp.) adapted for mice. Values of the respective limits of assay sensitivities were assigned to samples with undetectable TSH and T4 concentration.

Immunohistochemistry. Six-micrometer sections were subjected to antigen retrieval, incubated with pERK1/2 (Thr202/Tyr204) and pAKT (Ser473) antibodies (Cell Signaling), and counterstained with hematoxylin. SA-β-galactosidase activity was detected using a commercially available kit (Cell Signaling).

Cells, treatments, and proliferation analysis. Several independent cell lines were established from primary thyroid tumors developed by $Pten^{L/L}$;$Kras^{G12D}$ double-mutant (DM) mice[5] and grown in DMEM/10% fetal bovine serum. Pharmacologic inhibitors of PI3K (LY294002, 30 μmol/L) and MAPK/extracellular signal-regulated kinase (ERK) kinase (MEK) 1 (PD98059, 50 μmol/L) were added 24 h after plating, in quadruplicate. At the indicated time points, cells were counted using a Beckman Coulter counter or harvested in RIPA buffer for protein analysis and in Trizol (Invitrogen) for RNA analysis.

Western blot analysis. Thyroids and cells were homogenized on ice in RIPA buffer supplemented with Complete protease inhibitor tablet (Roche). Western blot analysis was carried out on 20 to 40 μg proteins with the following antibodies: MEK, pMEK (Ser217/221), ERK1/2, pERK1/2 (Thr202/Tyr204) (Cell Signaling), and cyclin D1 (Becton Dickinson).

[5] K.A. Miller, manuscript in preparation.

Note: Supplementary data for this article are available at Cancer Research Online (http://cancerres.aacrjournals.org/).

Requests for reprints: Antonio Di Cristofano, Department of Developmental and Molecular Biology, Albert Einstein College of Medicine, Price Center for Genetic and Translational Medicine, 1301 Morris Park Avenue, Room 302, Bronx, NY 10461. Phone: 718-678-1137; Fax: 718-678-1020; E-mail: adicrist@aecom.yu.edu.

doi:10.1158/0008-5472.CAN-09-0024

Real-time PCR. Total RNA was extracted with Trizol and reverse transcribed using the Thermoscript kit (Invitrogen). qRT-PCR was performed on an ABI-7900 using TaqMan Master mix and primers (Applied Biosystems). Each sample was run in triplicate and β-actin was used to control for input RNA. Data analysis was based on the Ct method, and experiments were repeated at least thrice using at least two independent pools.

The RT^2 Profiler Mouse MAPK PCR Array (SA Biosciences), containing 84 genes related to the MAPK pathway, plus housekeeping genes and controls, was used to analyze MAPK-related gene expression in the thyroids. Total RNA from pools of three to five mice was extracted with Trizol and further purified using the RNeasy Mini kit (Quiagen). RNA was reverse-transcribed with the First Strand kit (SA Biosciences), combined with the SYBR Green/ROX PCR master mix (SA Biosciences), and added to each well of the RT^2 Profiler PCR plate, containing the predispensed gene-specific primer sets. The reaction was run on an ABI-7900. Data analysis was based on the Ct method, with normalization to four different housekeeping genes, on quadruplicate samples from two independent thyroid pools.

Statistical analysis. Experiments were performed at least thrice. Data were analyzed using the JMP 5.1 software package. Differences with P values of 0.05 were considered statistically significant.

Results

To investigate the role of Ras in the pathogenesis of thyroid cancer, we have generated a mouse strain in which an oncogenic Kras mutant allele, G12D, is conditionally expressed in the thyroid epithelium through Cre-mediated deletion of a floxed STOP cassette preventing *KrasG12D* expression. This allele is targeted to its endogenous genomic locus, thus yielding physiologic expression levels of the mutant transcript (9). Tissue specificity is dictated by the human TPO, driving Cre expression in the follicular cells starting at day 14.5 of embryonic development (10).

TPO-Cre efficiently excised the STOP cassette (Supplementary Fig. S1*A*), leading to the expression of the oncogenic allele at endogenous levels. *Kras* mutant mice were born at the expected Mendelian frequencies and, throughout their lives, were indistinguishable from their wild-type littermates. Surprisingly, constitutive activation of Kras did not lead to morphologic (Fig. 1*A*) or functional (Fig. 2*A*) alterations of the thyroid gland, at least up to age 1 year. This result is in striking contrast with the ability of the

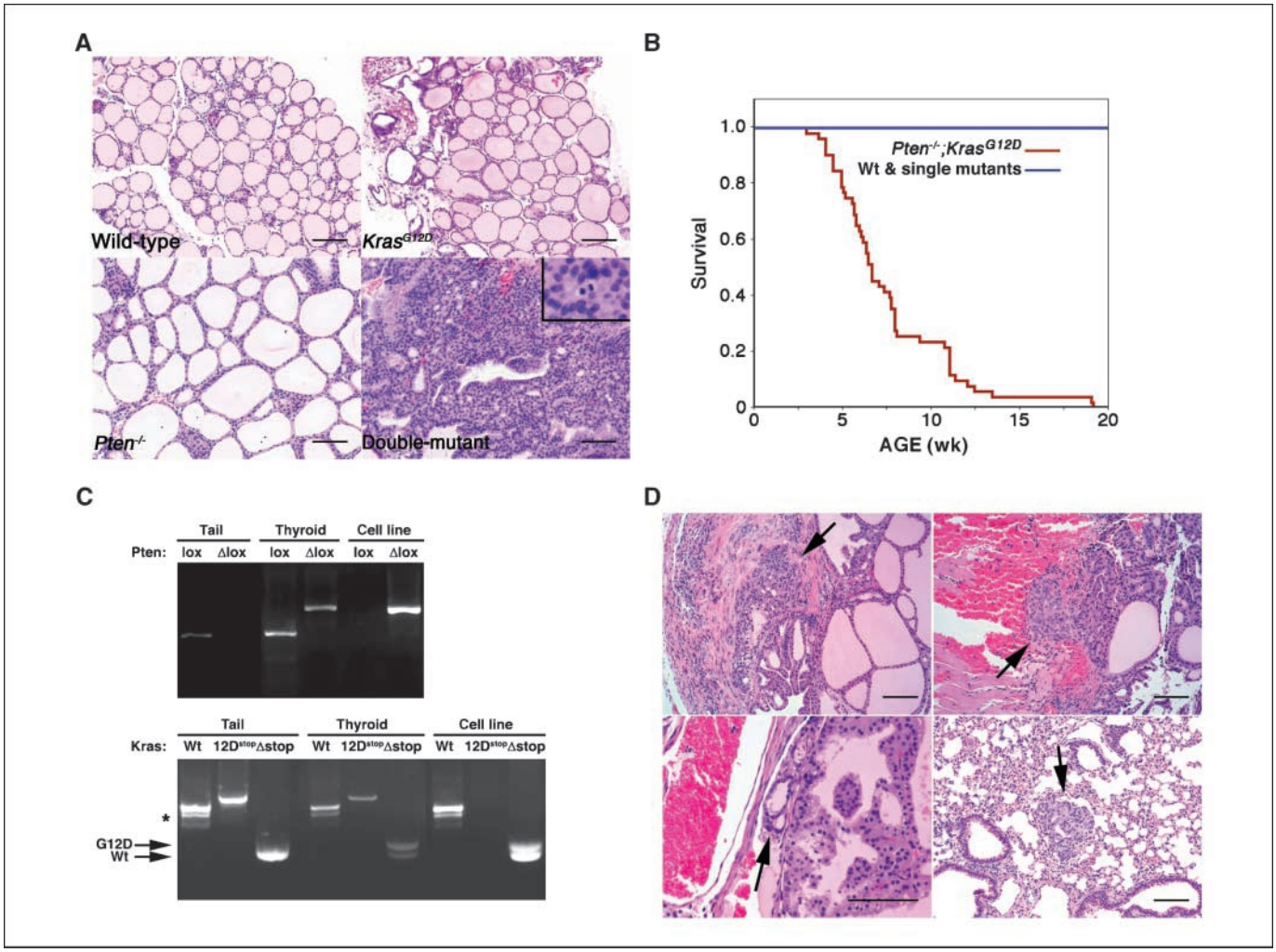

Figure 1. Simultaneous PI3K and Kras activation transforms thyrocytes. *A,* histopathology of thyroids from 12-wk-old mice. Note the normal follicles in *Kras^{G12D}* mice, compared with the hyperplasia in *Pten$^{-/-}$* mutants and the solid lesion with mitotic figures (*inset*) in DM mice. *Bar,* 100 μm. *B,* Kaplan-Meyer analysis of DM survival, compared with wild-type and single-mutant controls (n = 52 per group). *C,* PCR analysis demonstrating the recombinations leading to *Pten* deletion (*top*) and *Kras^{G12D}* activation (*bottom*). Separate PCRs on DNA from tail, thyroid, and tumor-derived cell lines were used to amplify unrecombined (*lox*) and recombined (*Δlox*) *Pten* alleles, as well as wild-type *Kras* allele (*wt*), unrecombined G12D allele carrying the STOP cassette (*12Dstop*), and recombined G12D allele (*Δstop*). *, an unspecific product. *D,* histopathologic features of thyroid carcinomas developing in DM mice: *top left,* capsular invasion (*arrow*); *top right,* muscle invasion (*arrow*); *bottom left,* vascular invasion (*arrow*); *bottom right,* lung metastasis (*arrow*).

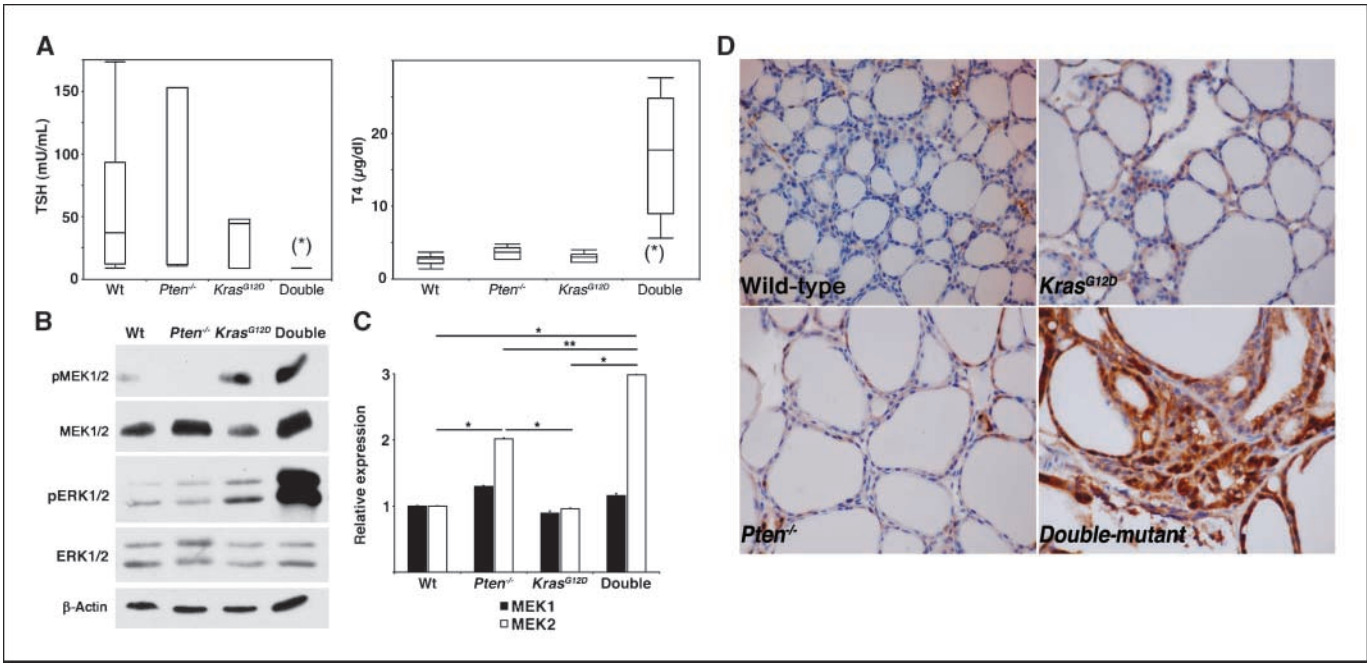

Figure 2. Hormonal and molecular characterization of mutant strains. *A,* TSH and T4 levels in 6- to 12-wk-old mice (n = 8–15), shown as box plots. The ends of the box are the 25th and 75th quantiles. The line across the box identifies the median value. Whiskers extend to the outermost data point. *, $P < 0.05$, Student's t test. *B,* Western blot analysis of MEK and ERK activation in pooled thyroids, normalized to β-actin. *C,* qRT-PCR analysis of Mek1 and Mek2 thyroid expression in mice of the four different genotypes. *, $P < 0.05$; **, $P > 0.05$. *D,* immunohistochemical detection of ERK1/2 phosphorylation, showing the cooperative effect of PI3K and Kras activation. Original magnification, ×200.

same allele to induce pancreatic intraepithelial neoplasia by age 2 weeks (13), colonic hyperplasia 2 weeks after activation (14), and lung hyperplasia 2 weeks after activation (9).

Ras activation, in certain cell types, leads to a negative feedback that down-regulates MAPK signaling and may induce senescence (15–17). On the other hand, genetic (7, 8) and epigenetic (18) alterations causing the activation of the PI3K pathway have recently been identified in most thyroid cancers. Thus, in thyroid follicular cells, *Kras* activating mutations might need the simultaneous activation of PI3K signaling to fully realize their oncogenic potential.

To test this hypothesis, we crossed the $Kras^{G12D}$;TPO-Cre mice with $Pten^{L/L}$;TPO-Cre mice, which have hyperplastic thyroids as a result of constitutively active PI3K signaling (Supplementary Fig. S1*B*; Fig. 1*A*), and progress to develop adenomas by age 10 months (19, 20). Strikingly, all the double-mutant (DM) mice rapidly developed thyroid follicular carcinomas (Fig. 1*A*). Fifty percent of the mice died within 7 weeks from birth, and none survived over age 4 months (Fig. 1*B*). These mice developed thyroids 200- to 500-fold larger than control glands (data not shown). PCR analysis showed that both the *Pten* and the *Kras* locus had undergone appropriate Cre-mediated recombination (Fig. 1*C*). Accordingly, follicular cells in both $Pten^{-/-}$ and $Kras^{G12D}$ glands showed dramatically increased pAKT levels (Supplementary Fig. S1*B*). Histopathology of the DM mice revealed that 30% to 90% of the thyroid glands was replaced by microfollicular to solid areas (Supplementary Fig. S2) presenting many hallmarks of thyroid follicular cancer, including capsular, muscle, and vascular invasion. In addition, all the mice surviving at least 12 weeks had developed thyroglobulin-positive lung metastases (Supplementary Fig. S3; Fig. 1*D*).

To assess the thyroid functional status in the four strains, and to determine whether the tumors depend on TSH signaling, we measured TSH and T4 in the serum of control and mutants. Although single gene mutation did not alter the levels of either hormone, TSH was drastically reduced and T4 increased in the DM mice, suggesting that simultaneous PI3K and Kras activation may confer a certain degree of thyroid autonomy (Fig. 2*A*). Although we still do not know the basis for this TSH-independent thyroid hormone synthesis, TSH suppression strongly suggests that tumor development, in this model, does not rely on TSH-mediated proliferative signals.

In several mouse models, endogenous Kras activation seems to be unable to fully activate MAPK signaling (4, 14). We analyzed the phosphorylation of MEK and its direct target ERK in the thyroids of the four strains. PI3K activation in $Pten^{-/-}$ thyroids did not alter the phosphorylation of these kinases. Surprisingly, although oncogenic Kras, alone, substantially increased MEK phosphorylation, this had no significant effect on ERK activation (Fig. 2*B* and *D*). Conversely, simultaneous activation of Kras and PI3K increased MEK phosphorylation at levels similar to oncogenic Kras alone, but, in this case, also drastically increased ERK phosphorylation, strongly suggesting that, at least in thyroid cells, PI3K signaling removes or overcomes a negative feedback uncoupling MEK and ERK activation. In addition, PI3K signaling increased MEK protein levels (Fig. 2*B*), and specifically MEK2 mRNA (Fig. 2*C*), providing an additional possible mechanism for ERK activation in the DM mice.

We used cell lines generated from DM tumors and pharmacologic inhibitors of PI3K (LY294002) and MEK1 (PD98059) to further investigate the cooperation between PI3K- and Kras-dependent signaling. Although MEK inhibition could decrease only to a certain degree the growth rate of the DM cells, targeting PI3K was much more effective, and the two compounds cooperated to completely inhibit the tumor cell growth (Fig. 3*A*).

Strikingly, we found that protracted PI3K inhibition in tumor-derived cells reduced ERK phosphorylation to the same extent as

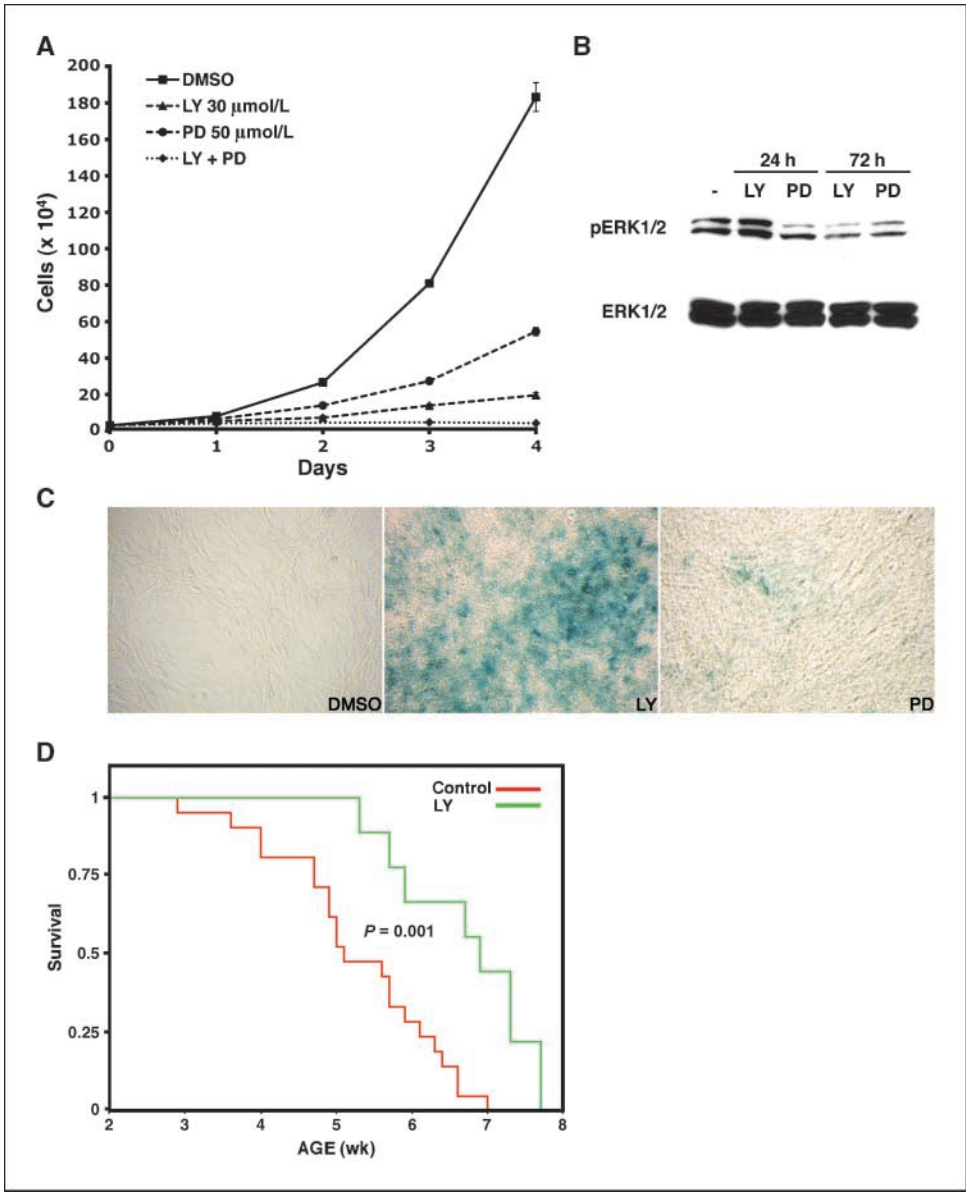

Figure 3. Modulation of PI3K signaling reduces cell proliferation *in vitro* and *in vivo*. *A,* growth curve of tumor cells upon treatment with LY294002 and PD98059. The graph represents one of at least four independent experiments, on three different cell lines. *B,* Western blot analysis of ERK1/2 activation upon PI3K or MEK pharmacologic inhibition. *C,* PI3K inhibition allows activated Kras to induce senescence in tumor-derived cell lines. The panels show a representative experiment (of 3 independent experiments, on different cell lines) using 10 μmol/L LY and 50 μmol/L PD for 6 d. *D, in vivo* administration of 25 mg/kg LY294002 prolongs the survival of DM mice (n = 9 LY-treated and 15 controls).

direct MEK inhibition (Fig. 3*B*), and led to the establishment of senescence (Fig. 3*C*), strongly suggesting that activation of Kras alone is not transforming because of a PI3K-sensitive negative feedback that uncouples MEK and ERK, terminates the MAPK cascade, and establishes senescence.

To test *in vivo* the permissive role of PI3K in Kras-dependent transformation, we administered LY294002 twice a week to DM mice at a low dose of 25 mg/kg (21), starting at age 3 weeks. PI3K inhibition significantly prolonged the survival of LY-treated mice, compared with untreated mice (Fig. 3*D*). These data are consistent with the results obtained on the tumor-derived cell lines, and support the notion that continuous PI3K signaling is necessary to permit the transforming activity of oncogenic Kras mutations.

We then used a qRT-PCR array to measure the expression of 84 genes associated with MAPK signaling in thyroid RNA from the 4 strains, trying to identify relevant targets of the cooperation between PI3K and Kras. Analysis of the expression of these genes identified a subgroup of transcripts specifically up-regulated in the DM mice, compared with wild-type thyroids (Fig. 4*A*). We have initially focused on these genes as prime candidates to mediate the combined transforming activity of PI3K and Kras, and in particular on cyclin D1.

Cyclin D1 transcript levels were up-regulated over 4-fold in the compound mutants, compared with both wild-type and single-mutant mice (Fig. 4*B*). In contrast, the expression levels of the other D-type cyclins, D2 and D3, were not significantly altered in any of the mutant strains. Accordingly, when we inhibited PI3K and/or MAPK signaling in tumor-derived cell lines, cyclin D1 transcript levels (but not D2 or D3) were down-regulated (again, ~4-fold) by simultaneous LY294002 and PD98059 treatment (Fig. 4*C*), thus validating our data obtained *in vivo*. Finally, we used Western blot analysis to prove that cyclin D1 protein expression followed the same pattern observed at the mRNA level. DM thyroids expressed much higher cyclin D1 protein than any of the single-mutant strains, and simultaneous PI3K and MAPK inhibition dramatically reduced cyclin D1 protein levels in tumor-derived cell lines (Fig. 4*D*).

Discussion

Expression of oncogenic Kras at physiologic levels using the $Kras^{LSL}$ mouse model (9) invariably results in the development of hyperplastic lesions that often progress and transform into carcinomas. For example, Kras activation in the lungs through intranasal instillation of Cre-expressing adenoviral vectors results in the development of hyperplasia as early as 4 days after activation (4) and adenocarcinomas by age 16 weeks (9). Similarly, expression of endogenous $Kras^{G12D}$ in the exocrine pancreas induces intraepithelial neoplasms by age 2 weeks and carcinomas after 6 months (13). It was thus surprising to find that oncogenic Kras activation in the thyroid follicular cells did not lead to any morphologic and functional alterations of the thyroid gland. Although it is possible that the strain in which these experiments have been performed (129Sv) harbors genetic modifiers of Kras activity not present in the strain used in the previous reports, it is more likely that the thyroid has specific mechanisms in place to limit the effect of oncogenic Kras mutations, and leading to a senescence-like state through the up-regulation of known negative regulators of oncogenic Ras including Sprouty-2 (17), dual-specificity phosphatases (22), and Ras-GAPs (15).

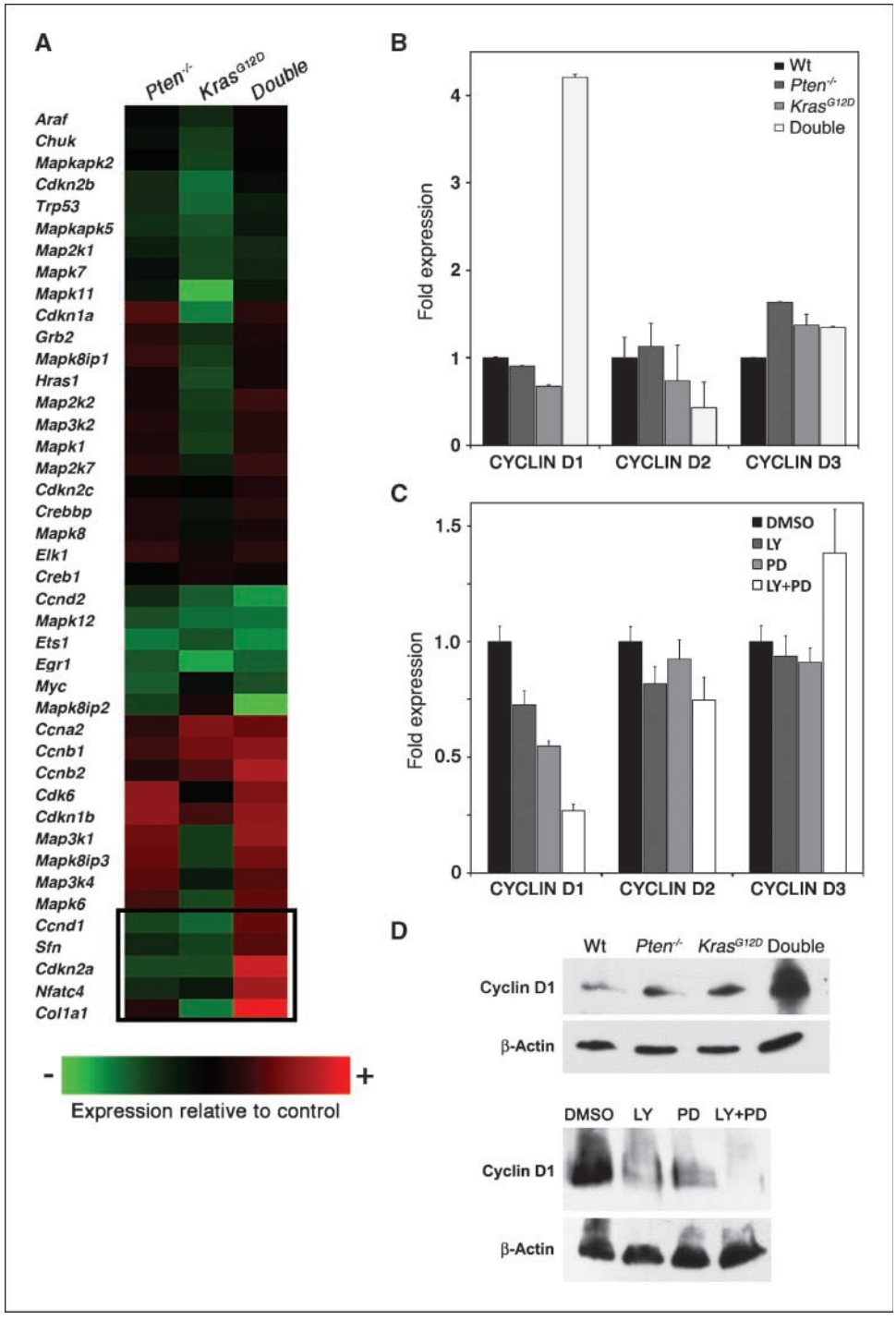

Figure 4. Cyclin D1 is a target of PI3K and Kras cooperation. *A,* heat map showing the expression of significantly deregulated genes in the thyroids of mutant mice, relative to controls. The group of genes cooperatively up-regulated by PI3K and Kras activation is boxed. *B,* qRT-PCR analysis of the expression of D-type cyclins in the thyroid of mice of the four different genotypes. *C,* simultaneous inhibition of PI3K and MAPK in DM cells for 48 h reduces cyclin D1 mRNA levels. *D,* Western blot analysis of cyclin D1 in protein extracts from thyroids (*top*), and tumor-derived cell lines treated for 48 h.

The finding that PI3K activation through loss of *Pten* is able to unleash the full oncogenic potential of the $Kras^{G12D}$ allele strongly suggests that PI3K may oppose such negative feedbacks, possibly through direct regulation of the expression level or enzymatic activity of these molecules.

As a result, we show that simultaneous activation of PI3K and Kras leads to the up-regulation of a group of genes that likely play an active role in the transformation process, similar to what has been recently described by Iwanaga and colleagues (23) in an analogous model of accelerated lung tumorigenesis. Although it is not surprising to find, among these culprits, Cyclin D1, a shared target of both Kras (24) and PI3K (25), from a biological standpoint, it is more puzzling the presence of *Cdkn2a*. Although it is possible that p14/p16 up-regulation represents an attempt of thyrocyte to counter the hyperproliferative signals generated by Kras and PI3K, additional studies are warranted to fully understand this finding. Nonetheless, it is worthy of note that *CDKN2A* up-regulation has been frequently reported in thyroid carcinomas (26–28).

In conclusion, using the mouse thyroid as a model system, our studies have uncovered a tight dependence of Kras transforming ability, *in vivo*, on constitutive PI3K signaling, which is required to allow full MAPK activation and cyclin D1 overexpression. Ongoing studies will address both the mechanistic details of this cooperative signaling, and the identity of additional clinically and therapeutically relevant targets.

Disclosure of Potential Conflicts of Interest

No potential conflicts of interest were disclosed.

Acknowledgments

Received 1/6/09; revised 1/29/09; accepted 2/16/09; published OnlineFirst 4/7/09.

Grant support: Fox Chase Cancer Center Core grant by the AECC Core grant and by NIH grants (CA97097 and CA128943; A. Di Cristofano) and (DK15070 and DK20595; S. Refetoff).

The costs of publication of this article were defrayed in part by the payment of page charges. This article must therefore be hereby marked *advertisement* in accordance with 18 U.S.C. Section 1734 solely to indicate this fact.

We thank Dr. Tyler Jacks for the $Kras^{LSL}$ mice; the Transgenic, Laboratory Animal, Biomarker, and Histopathology facilities of Fox Chase Cancer Center, and the Animal Facility of Einstein.

References

1. Shi YF, Zou MJ, Schmidt H, et al. High rates of ras codon 61 mutation in thyroid tumors in an iodide-deficient area. Cancer Res 1991;51:2690–3.
2. Vitagliano D, Portella G, Troncone G, et al. Thyroid targeting of the N-ras(Gln61Lys) oncogene in transgenic mice results in follicular tumors that progress to poorly differentiated carcinomas. Oncogene 2006;25:5467–74.
3. Feunteun J, Michiels F, Rochefort P, et al. Targeted oncogenesis in the thyroid of transgenic mice. Horm Res 1997;47:137–9.
4. Tuveson DA, Shaw AT, Willis NA, et al. Endogenous oncogenic K-rasG12D stimulates proliferation and widespread neoplastic and developmental defects. Cancer Cell 2004;5:375–87.
5. Pandey J, Umphress SM, Kang Y, et al. Modulation of tumor induction and progression of oncogenic K-ras-positive tumors in the presence of TGF- b1 haploinsufficiency. Carcinogenesis 2007;28:2589–96.
6. Kirsch DG, Dinulescu DM, Miller JB, et al. A spatially and temporally restricted mouse model of soft tissue sarcoma. Nat Med 2007;13:992–7.
7. Wang Y, Hou P, Yu H, et al. High prevalence and mutual exclusivity of genetic alterations in the phosphatidylinositol-3-kinase/akt pathway in thyroid tumors. J Clin Endocrinol Metab 2007;92:2387–90.
8. Hou P, Liu D, Shan Y, et al. Genetic alterations and their relationship in the phosphatidylinositol 3-kinase/Akt pathway in thyroid cancer. Clin Cancer Res 2007;13:1161–70.
9. Jackson EL, Willis N, Mercer K, et al. Analysis of lung tumor initiation and progression using conditional expression of oncogenic K-ras. Genes Dev 2001;15:3243–8.
10. Kusakabe T, Kawaguchi A, Kawaguchi R, Feigenbaum L, Kimura S. Thyrocyte-specific expression of Cre recombinase in transgenic mice. Genesis 2004;39:212–6.
11. Trotman LC, Niki M, Dotan ZA, et al. Pten dose dictates cancer progression in the prostate. PLoS Biol 2003;1:385–96.
12. Pohlenz J, Maqueem A, Cua K, Weiss RE, Van Sande J, Refetoff S. Improved radioimmunoassay for measurement of mouse thyrotropin in serum: strain differences in thyrotropin concentration and thyrotroph sensitivity to thyroid hormone. Thyroid 1999;9:1265–71.
13. Hingorani SR, Petricoin EF, Maitra A, et al. Preinvasive and invasive ductal pancreatic cancer and its early detection in the mouse. Cancer Cell 2003;4:437–50.
14. Haigis KM, Kendall KR, Wang Y, et al. Differential effects of oncogenic K-Ras and N-Ras on proliferation, differentiation and tumor progression in the colon. Nat Genet 2008;40:600–8.
15. Courtois-Cox S, Genther Williams SM, Reczek EE, et al. A negative feedback signaling network underlies oncogene-induced senescence. Cancer Cell 2006;10:459–72.
16. Macrae M, Neve RM, Rodriguez-Viciana P, et al. A conditional feedback loop regulates Ras activity through EphA2. Cancer Cell 2005;8:111–8.
17. Shaw AT, Meissner A, Dowdle JA, et al. Sprouty-2 regulates oncogenic K-ras in lung development and tumorigenesis. Genes Dev 2007;21:694–707.
18. Hou P, Ji M, Xing M. Association of PTEN gene methylation with genetic alterations in the phosphatidylinositol 3-kinase/AKT signaling pathway in thyroid tumors. Cancer 2008;113:2440–7.
19. Yeager N, Brewer C, Cai KQ, Xu XX, Di Cristofano A. mTOR is the key effector of PI3K-initiated proliferative signals in the thyroid follicular epithelium. Cancer Res 2008;68:444–9.
20. Yeager N, Klein-Szanto A, Kimura S, Di Cristofano A. Pten loss in the mouse thyroid causes goiter and follicular adenomas: insights into thyroid function and Cowden disease pathogenesis. Cancer Res 2007;67:959–66.
21. Bondar VM, Sweeney-Gotsch B, Andreeff M, Mills GB, McConkey DJ. Inhibition of the phosphatidylinositol 3′-kinase-AKT pathway induces apoptosis in pancreatic carcinoma cells *in vitro* and *in vivo*. Mol Cancer Ther 2002;1:989–97.
22. Owens DM, Keyse SM. Differential regulation of MAP kinase signalling by dual-specificity protein phosphatases. Oncogene 2007;26:3203–13.
23. Iwanaga K, Yang Y, Raso MG, et al. Pten inactivation accelerates oncogenic K-ras-initiated tumorigenesis in a mouse model of lung cancer. Cancer Res 2008;68:1119–27.
24. Lavoie JN, L'Allemain G, Brunet A, Muller R, Pouyssegur J. Cyclin D1 expression is regulated positively by the p42/p44MAPK and negatively by the p38/HOGMAPK pathway. J Biol Chem 1996;271:20608–16.
25. Bellacosa A, Kumar C, Di Cristofano A, Testa JR. Activation of AKT Kinases in Cancer: Implications for Therapeutic Targeting. Adv Cancer Res 2005;94:29–86.
26. Zafon C, Obiols G, Castellvi J, Ramon y Cajal S, Baena JA, Mesa J. Expression of p21cip1, p27kip1, and p16INk4a cyclin-dependent kinase inhibitors in papillary thyroid carcinoma: correlation with clinicopathological factors. Endocr Pathol 2008;19:184–9.
27. Ferru A, Fromont G, Gibelin H, et al. The status of CDKN2A α (p16INK4A) and β (p14ARF) transcripts in thyroid tumour progression. Br J Cancer 2006;95:1670–7.
28. Ball E, Bond J, Franc B, Demicco C, Wynford-Thomas D. An immunohistochemical study of p16(INK4a) expression in multistep thyroid tumourigenesis. Eur J Cancer 2007;43:194–201.